Mon. Not. R. Astron. Soc. **372,** 1799–1803 (2006) doi:10.1111/j.1365-2966.2006.10992.x

Gemini spectra of 12 000 K white dwarf stars*

S. O. Kepler,[1]† B. G. Castanheira,[1] A. F. M. Costa[1] and D. Koester[2]

[1] *Instituto de Física, Universidade Federal do Rio Grande do Sul, 91501-900 Porto-Alegre, RS, Brazil*
[2] *Institut für Theoretische Physik und Astrophysik, Universität Kiel, 24098 Kiel, Germany*

Accepted 2006 August 22. Received 2006 August 21; in original form 2006 July 19

ABSTRACT

We report signal-to-noise ratio (S/N) $\simeq$ 100 optical spectra for four DA white dwarf stars acquired with the GMOS spectrograph of the 8-m Gemini north telescope. These stars have $18 < g < 19$ and are around $T_{\rm eff} \sim 12\,000$ K, where the hydrogen lines are close to maximum. Our purpose is to test if the effective temperatures and surface gravities derived from the relatively low-S/N ($\langle$S/N$\rangle \approx 21$) optical spectra acquired by the Sloan Digital Sky Survey through model atmosphere fitting are trustworthy. Our spectra range from 3800 to 6000 Å, therefore including Hβ to H9. The H8 line was only marginally present in the SDSS spectra, but is crucial to determine the gravity. When we compare the values published by Kleinman et al. and Eisenstein et al. with our line-profile technique (LPT) fits, the average differences are: $\Delta T_{\rm eff} \simeq 320$ K, systematically lower in the SDSS, and Δ log $g \simeq 0.24$ dex, systematically larger in the SDSS. The correlation between the gravity and the effective temperature can only be broken at wavelengths bluer than 3800 Å. The uncertainties in $T_{\rm eff}$ are 60 per cent larger, and in log g larger by a factor of 4, than the internal uncertainties of Kleinman et al. and Eisenstein et al.

Key words: techniques: spectroscopic – white dwarfs.

1 INTRODUCTION

Kleinman et al. (2004) published the spectra of 2551 white dwarf stars in the Sloan Digital Sky Survey (SDSS) Data Release 1 (DR1), increasing the number of spectroscopically identified stars by almost 50 per cent compared to McCook & Sion (2003). Eisenstein et al. (2006) extended the white dwarf spectroscopic identification to DR4 with 9316 white dwarf stars reported. They fit their observed optical spectra from 3800 to 7000 Å to a grid of synthetic spectra derived from model atmosphere with ML2/$\alpha = 0.6$ convective transport in LTE, calculated by Detlev Koester. Their fits are for the whole spectra and photometry, allowing a reflux of the models according to a low-order polynomial, to incorporate effects of unknown reddening. The SDSS spectra have mean signal-to-noise ratio S/N (g) $\approx$13, and $\approx$21 for stars brighter than $g = 19$.

Starting with Schulz & Wegner (1981), most of the white dwarf spectra fits for $T_{\rm eff}$ and log g are values derived from the line profiles alone, if a sufficient set of lines is measured. Bergeron et al. (1995) showed S/N $\geqslant$ 70 is required for uncertainties $\Delta T_{\rm eff} \leqslant 300$ K. The low-order lines are temperature sensitive, and the higher order lines are pressure – therefore gravity – sensitive, as they weaken with increasing gravity; their line profiles are dominated by the quenching of the upper levels due to the high electronic density. However, these lines are also in the region where the atmospheric extinction is the largest and the CCD detectors the least sensitive.

The SDSS spectra have good flux calibration redwards of 4000 Å, but have a very low S/N below 4000 Å, even when the spectra extend to H8. Madej, Należyty & Althaus (2004) calculated the mass distribution for the DR1 SDSS DA sample and found that the mean mass increased below $T_{\rm eff} = 12\,000$ K, raising a doubt on the published values of Kleinman et al. (2004).

To test if the SDSS atmospheric values derived from the relatively low-S/N spectra are trustworthy, we obtained S/N $\approx$ 100 near 4500 Å for four DA white dwarf stars around $T_{\rm eff} = 12\,000$ K, listed in Table 1. We calculated the absolute magnitudes listed in the table from $T_{\rm eff}$ and log g obtained in their fits, convolving the synthetic spectra with the g-filter transmission curve and using the evolutionary models of Wood (1995) with C/O core, $M_{\rm He} = 10^{-2}\,M_*$, and $M_{\rm H} = 10^{-4}\,M_*$ to estimate their radius. The distances were then obtained from the distance moduli.

2 OBSERVATIONS

We used the Gemini Multi-Object Spectrograph (GMOS) on the 8-m Gemini north telescope, in the 1.5-arcsec long-slit mode, from

*Based on observations obtained at the Gemini Observatory, which is operated by the Association of Universities for Research in Astronomy, Inc., under a cooperative agreement with the NSF on behalf of the Gemini partnership: the National Science Foundation (United States), the Particle Physics and Astronomy Research Council (United Kingdom), the National Research Council (Canada), CONICYT (Chile), the Australian Research Council (Australia), CNPq (Brazil) and CONICET (Argentina).

†E-mail: kepler@if.ufrgs.br

© 2006 The Authors. Journal compilation © 2006 RAS

Downloaded from http://mnras.oxfordjournals.org/ at FundaÃ§Ã£o CoordenaÃ§Ã£o de AperfeiÃ§oamento de Pessoal de NÃ-vel Superior on February 26, 2014

Table 1. SDSS.

Spectra spSpec (MPF)	Name (SDSS)	g	M_g	$T_{\rm eff}$ (K)	$\sigma_{\rm T}{}^{a}$ (K)	log g	$\sigma_{\log g}{}^{a}$	Mass ($M_\odot$)	$\sigma_{\rm M}$ ($M_\odot$)	d (pc)
51929-0458-188	J030325.22−080834.9	18.74	12.58	11 418	119	8.500	0.070	0.925	0.040	171
52199-0681-079	J233454.17−001436.2	18.34	11.66	13 344	321	8.140	0.070	0.699	0.040	217
51818-0383-111	J232659.23−002348.0	17.50	12.53	10 622	47	8.330	0.040	0.815	0.020	99
51821-0384-008	J233647.01−005114.6	18.29	11.25	13 249	247	7.860	0.050	0.544	0.020	255

[a]The quoted uncertainties on all tables are the internal uncertainties of the fit only.

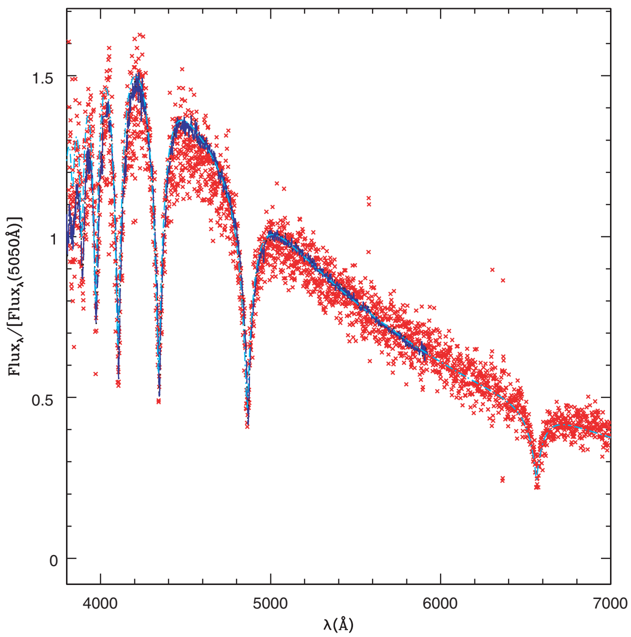

Figure 1. Gemini (solid dark line) and SDSS spectra (crosses) of WD J0303−0808, and the model fits (dashed lines). We plot both the best fit by the LPT (Table 2) and the whole spectra fitting (Table 3).

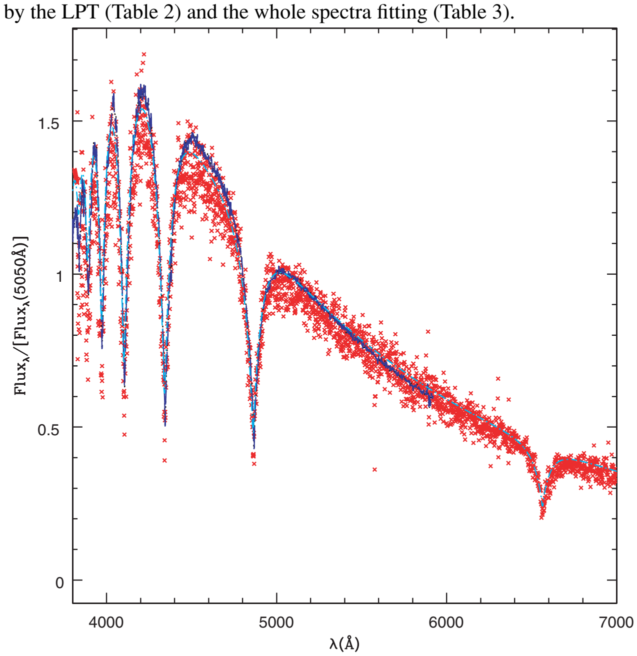

Figure 2. Gemini and SDSS spectra of WD J2334−0014, and the model fits.

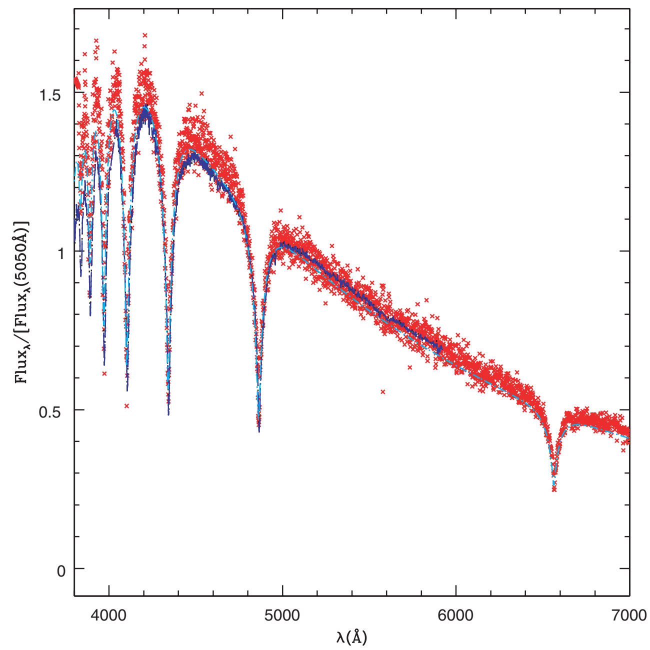

Figure 3. Gemini and SDSS spectra of WD J2326−0023, and the model fits.

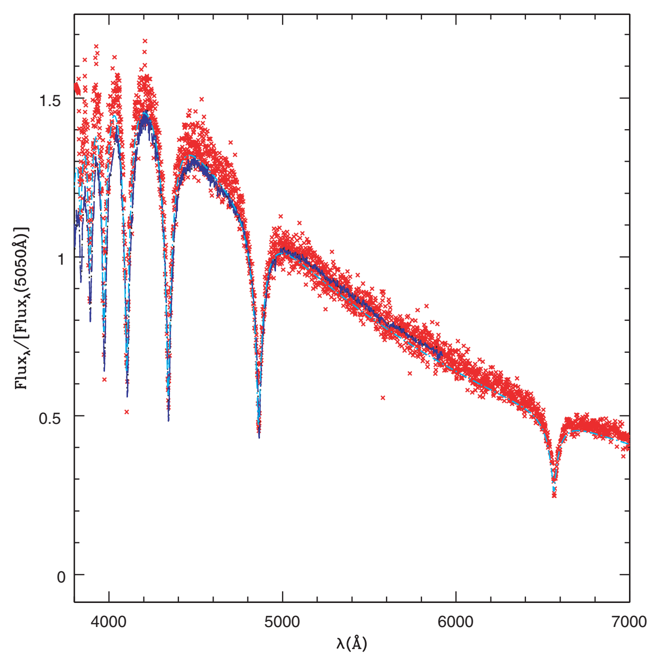

Figure 4. Gemini and SDSS spectra of WD J2336−0051, and the model fits.

Downloaded from http://mnras.oxfordjournals.org/ at FundaÃ§Ã£o CoordenaÃ§Ã£o de AperfeiÃ§oamento de Pessoal de NÃvel Superior on February 26, 2014

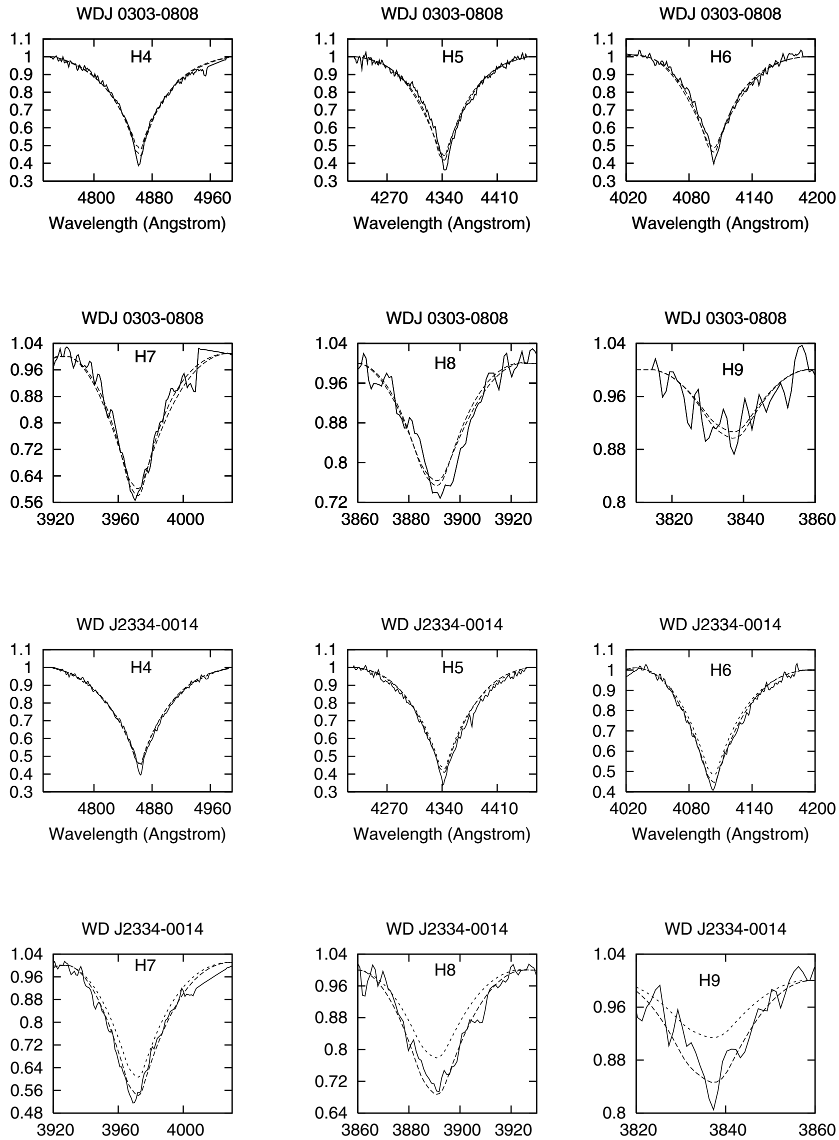

Figure 5. Line profiles in the Gemini spectra of WD J0303−0808 and WD J2334−0014, and the models fits. The models fitted by Kleinman et al. (2004) are the ones with higher gravities and therefore shallower lines, incompatible with the observed H9 profiles. Even though the lines were centred before fitting, we plot here the observed (uncentred) lines.

Table 2. $T_{\rm eff}$ and log g with ML2/$\alpha = 0.6$ using the line profile.

Name	$T_{\rm eff}$	$\sigma_{T_{\rm eff}}$	log g	$\sigma_{\log g}$	Mass	$\sigma_{\rm Mass}$	Age (Gyr)
WD J0303−0808	11 960	160	8.305	0.017	0.791	0.003	0.724
WD J2334−0014	13 543	118	7.864	0.037	0.535	0.003	0.284
WD J2326−0023	10 821	160	8.029	0.007	0.620	0.005	0.625
WD J2336−0051	13 797	21	7.712	0.009	0.461	0.005	0.223

Table 3. $T_{\rm eff}$ and log g with ML2/$\alpha = 0.6$ using the whole spectra.

Name	$T_{\rm eff}$	$\sigma_{T_{\rm eff}}$	log g	$\sigma_{\log g}$	Mass	$\sigma_{\rm Mass}$	Age(Gyr)
WD J0303−0808	11 423	112	7.821	0.016	0.506	0.010	0.434
WD J2334−0014	13 388	24	7.880	0.034	0.543	0.012	0.299
WD J2326−0023	10 467	404	7.800	0.012	0.492	0.012	0.535
WD J2336−0051	12 192	177	7.736	0.003	0.465	0.012	0.331

3800 to 6000 Å. We observed with the B600-G5303 grating and 2×2 binning, achieving 2.8-Å resolution.

The spectra are reduced with the Gemini/GMOS package in IRAF, calibrated with standard stars observed the same night as the targets and extinction corrected using Mauna Kea mean coefficients. The normal flux and extinction calibration was done with bins of 16 Å, leaving undulations in the spectra. As the resolution of our spectra is higher, we used a 1-Å calibration for the primary flux standard star G191−B2B, which has been fitted to white dwarf model atmospheres (Bohlin 2002), and an observation of the star with the same set-up used in our spectra, for a fine calibration.

3 MODELS AND FITTING

We employed a synthetic spectra grid similar to that used by Kleinman et al. (2004), but extended and denser, to prevent

© 2006 The Authors. Journal compilation © 2006 RAS, MNRAS **372,** 1799–1803

Downloaded from http://mnras.oxfordjournals.org/ at FundaÃ§Ã£o CoordenaÃ§Ã£o de AperfeiÃ§oamento de Pessoal de NÃvel Superior on February 26, 2014

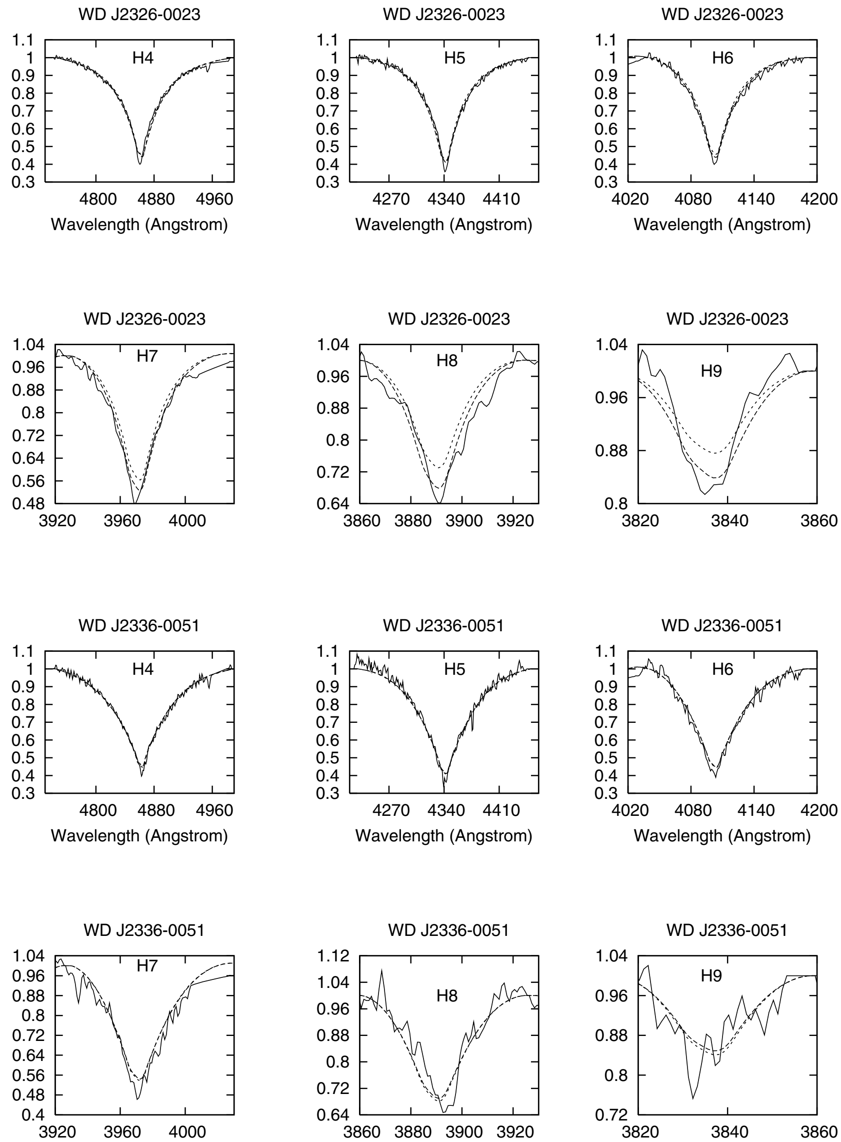

Figure 6. Line profiles in the Gemini spectra of WD J2326−0023 and WD J2336−0051, and the models fits. The models fitted by Kleinman et al. (2004) are the ones with higher gravities and therefore shallower lines, incompatible with the observed H9 profiles.

uncertainties in the fits to dominate the comparison. The choice of the ML2/$\alpha = 0.6$ parametrization for convection was demonstrated by Bergeron et al. (1995) to give internal consistency with the temperatures derived in the optical and the ultraviolet, photometry, parallax and gravitational redshift. It also gave the same mean mass for his sample with $T_{\rm eff}$ larger and smaller than 13 000 K, while other parametrizations did not. ML2 corresponds to the Bohm & Cassinelli (1971) description of the mixing-length theory and $\alpha = \ell/\lambda_P$ is the ratio of the mixing length to the pressure scaleheight.

For the line-profile technique (LPT) fitting, we normalize both the observed spectra and the models to a continuum set at a fixed distance from the line centre and recentre the observed lines to account for radial velocities and wavelength calibration uncertainties. The synthetic spectra are convolved with a Gaussian instrumental profile and the whole grid is fitted by least squares, weighting all the points equally. We fitted the spectra both whole spectra (Figs 1–4), and line profiles only (Figs 5 and 6), to compare with the values of Kleinman et al. (2004). The LPT fit does not require spectrophotometric quality data and is basically immune to flux calibration and reddening uncertainties. For the whole spectra fitting (all), we normalize the observations and the models in a region around 5050 Å.

We tested Seaton (1979) interstellar reddening proportional to the distances we measured and found no detectable difference. Even though the distances are slightly over 100 pc, the SDSS fields were selected perpendicularly to the galactic disk, so reddening should be low.

To test the fitting method, we simulated different noise levels added to synthetic spectra. By Monte Carlo simulations, we estimated the average uncertainties in both the techniques, LPT and all spectra fitting. As the S/N is varying from 100 at 4500 Å to less than 30 at 3800 Å, where the log g effects are the largest, we report the simulations up to S/N = 60, to reinforce the average over wavelength. The uncertainties in $T_{\rm eff}$ are listed in Table 4, and we conclude that the more trustworthy fits are when we fit all the spectra, if the uncertainties in flux calibration and interstellar reddening are not dominant.

© 2006 The Authors. Journal compilation © 2006 RAS,

Downloaded from http://mnras.oxfordjournals.org/ at FundaÃ§Ã£o CoordenaÃ§Ã£o de AperfeiÃ§oamento de Pessoal de NÃvel Superior on February 26, 2014

Table 4. Uncertainties fitting model with the simulated noise spectra.

S/N	$\sigma_{T_{\rm eff}}$ (all)	$\sigma_{\log g}$ (all)	$\sigma_{T_{\rm eff}}$ (LPT)	$\sigma_{\log g}$ (LPT)
10	1550	0.76	1910	0.36
20	745	0.16	1105	0.17
40	505	0.12	685	0.10
60	200	0.05	370	0.07

4 RESULTS AND DISCUSSIONS

(i) The effective temperatures derived by Kleinman et al. (2004) are trustworthy. The mean difference from the SDSS to our high-S/N spectra has $\Delta T_{\rm eff} = 320 \pm 200$ K, ($\Delta T_{\rm eff} = 370 \pm 230$ K including the variable WD J0303−0808) systematically lower in the SDSS, where the uncertainties were calculated adding quadratically the internal uncertainties of the fit.

(ii) The surface gravity uncertainties are underestimated by a factor of 4. The mean difference from the SDSS to our high-S/N spectra has $\Delta \log g = 0.24 \pm 0.08$, ($\Delta \log g = 0.24 \pm 0.06$ including the variable WD J0303−0808) systematically larger in the SDSS, which corresponds to $\Delta\mathcal{M} \simeq 0.13\ \mathcal{M}_{\odot}$ overestimate in mass.

The main difficulty in these fits is the correlation between the derived $T_{\rm eff}$ and $\log g$ – a small increase in $T_{\rm eff}$ can be compensated by a small decrease in $\log g$ – as for WD J0303−0808, for which the model with $T_{\rm eff} = 12\,000$ K, $\log g = 8.0$, from our LPT fit, differs from the whole spectra best fit $T_{\rm eff} = 11\,400$ K, $\log g = 8.3$ only below 3800 Å, where we have no measured flux.

The four stars reported here were classified as not-observed-to-vary (NOV) by Mukadam et al. (2004), but Castanheira et al. (2006) reported WD J0303−0808 is, in fact, a low-amplitude pulsator. Pulsation does introduce a real variation of the measured effective temperature of 50 to 500 K, depending on the real amplitude of the pulsation, during a cycle (Kepler 1984).

A systematic increase in the measured gravity for white dwarfs at effective temperatures lower than 12 000 K has been observed for more than a decade, and for the SDSS spectra has been reported by Kleinman et al. (2004), Madej et al. (2004) and Eisenstein et al. (2006). Our results indicate that such an increase, in the region of Balmer line maximum, $14\,000 \geqslant T_{\rm eff} \geqslant 11\,000$ K, is due to the projection of the $T_{\rm eff}$–$\log g$ real-correlated solution on to a smaller $T_{\rm eff}$ range. Such projection would also explain why Mukadam et al. (2004) and Mullally et al. (2005) found a narrower ZZ Ceti instability strip than Bergeron et al. (2004) and Gianninas, Bergeron & Fontaine (2005), but contaminated by non-variables.

ACKNOWLEDGMENT

Gemini GN-2005B-Q-67.

REFERENCES

Bergeron P., Wesemael F., Lamontagne R., Fontaine G., Saffer R. A., Allard N. F., 1995, ApJ, 449, 258
Bergeron P., Fontaine G., Billères M., Boudreault S., Green E. M., 2004, ApJ, 600, 404
Bohlin R. C., 2002, in Arribas S., Koekemoer A., Whitmore B., eds, The 2002 HST Calibration Workshop: Hubble After the Installation of the ACS and the NICMOS Cooling System. Space Telescope Science Institute, Baltimore, MD, p. 115
Bohm K. H., Cassinelli J., 1971, A&A, 12, 21
Castanheira B. G. et al., 2006, A&A, submitted
Eisenstein D. J. et al., 2006, ApJS, in press
Gianninas A., Bergeron P., Fontaine G., 2005, ApJ, 631, 1100
Kepler S. O., 1984, ApJ, 286, 314
Kleinman S. J. et al., 2004, ApJ, 607, 426
Madej J., Należyty M., Althaus L. G., 2004, A&A, 419, L5
McCook G. P., Sion E. M., 2003, VizieR Online Data Catalog, 3235, 1
Mukadam A. S. et al., 2004, ApJ, 607, 982
Mullally F., Thompson S. E., Castanheira B. G., Winget D. E., Kepler S. O., Eisenstein D. J., Kleinman S. J., Nitta A., 2005, ApJ, 625, 966
Schulz H., Wegner G., 1981, A&A, 94, 272
Seaton M. J., 1979, MNRAS, 187, 73P
Wood M. A., 1995, LNP Vol. 443: White Dwarfs, 443, 41

This paper has been typeset from a TEX/LATEX file prepared by the author.

Downloaded from http://mnras.oxfordjournals.org/ at FundaÃ§Ã£o CoordenaÃ§Ã£o de AperfeiÃ§oamento de Pessoal de NÃvel Superior on February 26, 2014